International Journal of Fracture **114:** 203–224, 2002.

The stress field in a [0°/90°] laminated composite plate containing a finite line crack

E.S. FOLIAS
Department of Mathematics, University of Utah, Salt Lake City, UT 84112, U.S.A.

Received 11 October 2000; accepted in revised form 7 January 2002

Abstract. This paper deals with the construction of an asymptotic solution for the stress field in a laminated composite plate, with [0/90] stacking sequence. The plate contains through the thickness a line crack of length 2c and its perimeter boundaries are sufficiently far away from the crack so that no edge effects are present. The stress field is derived explicitly, and includes a correction factor to account for the laminate effects in the third dimension. The stress σ_{zz} is a maximum at an angle of $\theta \approx 83°$ (see Figure 3). The stress field may now be used to bridge the gap between macro and micro mechanics and to derive a series of fracture criteria, at the micro and macro level, which ultimately will provide us with a better understanding of the formation of the damaged zone ahead of the crack tip. For example, the stress field is used to derive one such approximate fracture criterion for mode I loading and for a self similar type of fracture, similar to that of Griffith. This criterion shows how the periodic length of the material lay-up microstructure effects the fracturing characteristics of the material system. Comparison with some experimental observations for two different material systems shows a fairly good agreement which substantiates the predicted influence.

Key words: Cracked plate, fracture, laminated composite plate, 3D stress field, effect of thickness, effect of periodic length, self-similar fracture.

1. Introduction

Despite careful design, practically every structure contains stress risers due to the presence of inclusions, holes or cracks. Bolt holes and rivet holes are necessary components for structural joints. It is not surprising, therefore, that the majority of service cracks nucleate in the vicinity of a stress riser. While the subject of stress risers is certainly familiar to engineers, the situation is significantly more complex in the case of high-performance laminated composite materials. The presence of a hole or a crack in the laminate introduces significant stress contributions in the third dimension which create a very complicated three-dimensional (3-D) stress state in the vicinity of such discontinuities. Moreover, this complex state of stress may depend on the stacking sequence of the laminate, the fiber orientation of each lamina as well as the material properties of the fiber and of the matrix. Ultimately, these stress risers form a primary source of damage initiation and property degradation, particularly in the presence of cyclic loading. Experimental investigations carried out by Bakis and Stinchcomb (1986) on graphite-epoxy laminates which have been weakened by a circular hole give us a better insight of this damage growth development under the action of cyclic loading. In general, the progression of this damaged process may be characterized as (i) debonding along fiber-matrix interfaces, (ii) matrix cracking parallel to the fibers, (iii) matrix cracking between fibers, (iv) delamination along the interface of two adjacent laminae with different fiber orientations, and (v) fiber breakage.

Thus, if rational designs using fiber-reinforced-resin matrix composite laminates are to be made, their performance under static, dynamic, fatigue and environmental loads need to be predictable. The first step towards this goal is the realization that the ultimate failure, as well as many other aspects of the composite behavior, is the result of the growth and accumulation of microdamage to the fibers, matrix and their interfaces. Thus, it appears that any generally successful model of performance and failure must incorporate the effects of this damage in some way. This certainly represents a challenge. In this paper, we will address some simple forms of such damage, as related to that of crack initiation and possible delamination.

Delamination has long been recognized as one of the most important failure modes in laminated composite structures. The growth of a delamination may result in a substantial reduction of strength and stiffness of the laminate. The identification, therefore, of such locations in a composite structure is of great interest to the designer. Experimental studies by Pipes et al. (1973) have shown that the delamination mode of failure is most likely to initiate at the free edges. One conjectures, therefore, that the stresses at the intersection between a free edge and an interface may well be singular. Indeed, analytical investigations (Wang and Choi, 1982; Zwiers et al. 1982) on straight free edges show that a stress singularity exists for certain types of laminates.

Alternatively, a curved free edge is inherently a 3-D problem which presents greater mathematical difficulties. For this reason, past analyses have been based primarily on finite element methods with standard finite elements (Raju and Crews, 1982), as well as elements which incorporate the stress singularity in the formulation (Rybicki and Schmueser, 1978; Ericson et al. 1984). While such methods can provide us with stress trends in the boundary layer region, it is rather difficult to extract from them with certainty the order of the prevailing stress singularity that is present at the material interface. Moreover, experimental investigations carried out on straight edges by Pagano (1974) show that the laminate stacking sequence can indeed affect the static strength of the laminate. Similar experimental observations were also made by Daniel et al. (1974) on plates with circular holes. The subject, therefore, of stress risers due to holes and particularly due to cracks in the presence of periodic structures does warrant further investigation.

Thirteen years ago, Folias (1988a) investigated analytically the interlaminar stresses at the boundary layer in the vicinity of a free-edge and a hole, for two different isotropic materials. The analysis revealed that the stress field there possesses a weak singularity, that depends only on the material properties of the two adjacent laminates. Subsequently, Folias (1992) extended this analysis to also include transversely isotropic laminae of an arbitrary stacking sequence. This analysis revealed that the stress singularity in the latter case depends, not only on the material constants and the fiber orientations of the two adjacent laminae, but also on the polar angle θ.

In this paper an analytical method is developed in order to study the 3D stress field in a, cracked, laminated composite plate with a periodic stacking sequence of $[0^\circ/90^\circ]$. This particular stacking sequence is used in order to make the mathematical details of the paper a little easier to follow. The general method, however, exhibits a great deal of flexibility and can be used to solve a much larger class of mixed boundary value problems arising in the field of fracture of composite material systems. The method can also be extended to include cases where the cracks are neither parallel nor perpendicular to the direction of the fibers. Special attention is given to the stress field in the neighborhood of the crack front. Finally, one of the most important goals of this study is to assess what effect, if any, does the presence of a periodic length have on the fracturing characteristics of a cracked laminated composite

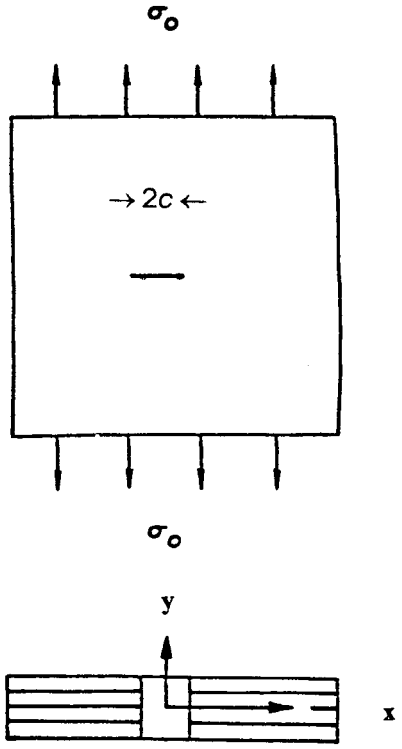

Figure 1. Laminated composite plate of arbitrary thickness and containing a crack.

material system. The author believes that such information is very important in trying to fully understand the failure mechanisms of composite material systems.

2. Formulation of the problem

Consider the equilibrium of a laminated composite plate that occupies the space $|x| < \infty$, $|z| < \infty$, $|y| < \infty$, and contains a finite line crack of length $2c$ along the direction of the x-axis. The plate consists of laminae made of transversely isotropic material with a $[0°/90°]_s$ stacking sequence. Far away from the crack, the plate is assumed to be subjected to a uniform, tensile, stress σ_0 along the direction of the z-axis and parallel to the bounding planes (Figure 1).

In the absence of body forces, the coupled differential equations governing the displacement functions u, v and w for a 0° layer are given by (Lekhnitskii, 1963):

$$C_{22}\frac{\partial^2 u}{\partial x^2}+(C_{22}-C_{44})\frac{\partial^2 v}{\partial x\partial y}+C_{13}\frac{\partial^2 w}{\partial x\partial z}+\frac{\partial}{\partial y}\left\{C_{44}\left(\frac{\partial u}{\partial y}+\frac{\partial v}{\partial x}\right)\right\}+C_{55}\left(\frac{\partial^2 u}{\partial z^2}+\frac{\partial^2 w}{\partial x\partial z}\right)=0, \quad (1)$$

$$C_{44}\left(\frac{\partial^2 u}{\partial x\partial y}+\frac{\partial^2 v}{\partial x^2}\right)+\frac{\partial}{\partial y}\left\{(C_{22}-C_{44})\frac{\partial u}{\partial x}+C_{22}\frac{\partial v}{\partial y}+C_{13}\frac{\partial w}{\partial z}\right\}+C_{55}\left(\frac{\partial^2 v}{\partial z^2}+\frac{\partial^2 w}{\partial y\partial z}\right)=0, \quad (2)$$

$$C_{55}\left(\frac{\partial^2 u}{\partial x\partial z}+\frac{\partial^2 w}{\partial x^2}\right)+\frac{\partial}{\partial y}\left\{C_{55}\left(\frac{\partial v}{\partial z}+\frac{\partial w}{\partial y}\right)\right\}+C_{13}\frac{\partial^2 u}{\partial x\partial z}+C_{13}\frac{\partial^2 v}{\partial y\partial z}+C_{11}\frac{\partial^2 w}{\partial z^2}=0, \quad (3)$$

where the C_{ij}'s represent the material stiffness constants for a layer whose fibers are running parallel to the z-axis.

The stress-strain relations, for a 0° layer are given by the constitutive relations :

$$\begin{bmatrix} \sigma_{xx} \\ \sigma_{yy} \\ \sigma_{zz} \\ \tau_{xy} \\ \tau_{yz} \\ \tau_{xz} \end{bmatrix} = \begin{bmatrix} C_{22} & C_{22}-2C_{44} & C_{13} & 0 & 0 & 0 \\ C_{22}-2C_{44} & C_{22} & C_{13} & 0 & 0 & 0 \\ C_{13} & C_{13} & C_{11} & 0 & 0 & 0 \\ 0 & 0 & 0 & C_{44} & 0 & 0 \\ 0 & 0 & 0 & 0 & C_{55} & 0 \\ 0 & 0 & 0 & 0 & 0 & C_{55} \end{bmatrix} \begin{bmatrix} \epsilon_{xx} \\ \epsilon_{yy} \\ \epsilon_{zz} \\ 2\epsilon_{xy} \\ 2\epsilon_{yz} \\ 2\epsilon_{xz} \end{bmatrix}. \tag{4}$$

Similarly, for the 90° layer, the corresponding governing equations, as well as the stress-strain relations, can be obtained from the above by a simple interchange of the appropriate axes.

As to the boundary conditions, we require that both shear stresses, i.e.,

$$\tau_{xz} = \tau_{yz} = 0; \quad \text{at} \quad z = 0, \text{ and for all } |x| < \infty, |y| < \infty, \tag{5}$$

and that the normal stress

$$\sigma_{zz} =; \quad \text{at} \quad z = 0, \text{ and for all } |x| < c, |y| < \infty. \tag{6}$$

Finally, far away from the crack, all displacements and stresses are assumed to be finite. Moreover, ahead of the crack prolongation, i.e., at $z = 0$ and for $|x| > c$, the material is assumed to be continuous.

It is found convenient at this point to seek the solution to the crack plate problem in the form

$$u = u^{(c)} + u^{(P)}, \text{ etc.}$$

which is characteristic to the solution of crack problems. The first component represents the 'complimentary' solution while the second component represents the usual 'undisturbed' or 'particular' solution of a plate without the presence of a crack.

3. Method of solution

The special case of a 3D homogeneous and isotropic, cracked, plate has been studied analytically by Folias (1975). Thus, motivated by these findings (see Equations (115)–(117) of the above reference, one may seek the solution of the 0° layer system (i.e., Equations (1)–(3) in the form:

$$u^{[0]} = \frac{\partial}{\partial x}\{f_1 + f_2\} - \frac{\partial}{\partial y}\{f_3\}, \tag{7}$$

$$v^{[0]} = \frac{\partial}{\partial y}\{f_1 + f_2\} + \frac{\partial}{\partial x}\{f_3\}, \tag{8}$$

$$w^{[0]} = \frac{\partial}{\partial z}\{m_1 f_1 + m_2 f_2\}, \tag{9}$$

where the constants m_1 and m_2 represent the roots of the algebraic equation

$$[C_{55}(C_{13}+C_{55})]m^2+[C_{55}^2+(C_{13}+C_{55})-C_{22}C_{11}]m+C_{55}(C_{13}+C_{55})=0 \tag{10}$$

and where the stress potentials f_1, f_2, f_3 satisfy the 3D, scaled, Laplace's equation

$$\frac{\partial^2 f_i}{\partial x^2}+\frac{\partial^2 f_i}{\partial y^2}+\epsilon_i^2\frac{\partial^2 f_i}{\partial z^2}=0; \quad i=1,2,3, \tag{11}$$

with

$$\epsilon_i=\sqrt{\frac{C_{55}+m_i(C_{13}+C_{55})}{C_{22}}}; \quad i=1,2 \quad \text{and} \quad \epsilon_3=\sqrt{\frac{C_{55}}{C_{44}}}. \tag{12}$$

Similarly, the solution for the 90° layer is sought also in the form

$$u^{[90]}=\frac{\partial}{\partial x}\{m_1\hat{f}_1+m_2\hat{f}_2\}, \tag{13}$$

$$v^{[90]}=\frac{\partial}{\partial y}\{\hat{f}_1+\hat{f}_2\}+\frac{\partial}{\partial z}\{\hat{f}_3\}, \tag{14}$$

$$w^{[90]}=\frac{\partial}{\partial z}\{\hat{f}_1+\hat{f}_2\}-\frac{\partial}{\partial y}\{\hat{f}_3\}, \tag{14}$$

where here again the stress potentials $\hat{f}_1$, $\hat{f}_2$, $\hat{f}_3$ satisfy the revised 3D, scaled, Laplace's equation

$$\epsilon_i^2\frac{\partial^2 f_i}{\partial x^2}+\frac{\partial^2 f_i}{\partial y^2}+\frac{\partial^2 f_i}{\partial z^2}=0; \quad i=1,2,3. \tag{16}$$

Thus, the coupled governing equations have been uncoupled and furthermore reduced to that of constructing a solution to a, 3D, Laplace's equation.

4. A particular material

As a practical matter, we consider the material Hercules AS4/3501-6. This material is made of thin carbon fibers (approximately 10 μm or 0.001 cm in diameter) which are placed in an epoxy prepreg and pressed into thin sheets, with all the fibers running in one direction. The sheets are then stacked so that in each layer the fibers run perpendicularly to the fibers of the previous layer. The sheets are then heated and pressed together, so that the epoxy forms a continuous matrix that holds the fibers together. The resulting plate is of the form $\ldots 0°/90°/0°/90° \ldots$. (see Figure 2). Moreover, each layer is quite thin (approx. 127 μm), and a plate of this material, of one quarter inch thick, contains approximately 25 layers.

Let us consider, therefore, such a composite plate that is made of alternating layers, with layer 1 having fibers which run along the z-direction, and with layer 2 having fibers which run along the x-direction. The resulting C_{ij} coefficients for this material system have been found experimentally as

$$\begin{aligned} C_{11}&=20.830, & C_{55}&=0.710,\\ C_{22}&=\ 1.651, & C_{12}&=0.647,\\ C_{44}&=\ 0.502, & C_{13}&=0.623. \end{aligned} \tag{17}$$

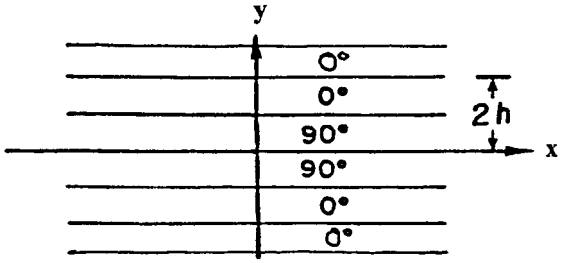

Figure 2. Material lay-up of high temperature carbon/epoxy composite.

in million pounds (force) per square inch.

Thus, the governing equations describing the material behavior for layer 1 become

$$\partial_1\{C_{22}\epsilon_{11} + (C_{22} - 2C_{44})\epsilon_{22} + C_{13}\epsilon_{13}\} + 2\partial_2\{C_{44}\epsilon_{12}\} + 2\partial_3\{C_{55}\epsilon_{13}\} = 0, \tag{18}$$

$$2\partial_1\{C_{44}\epsilon_{12}\} + 2\partial_2\{(C_{22} - 2C_{44})\epsilon_{11} + C_{22}\epsilon_{22} + C_{13}\epsilon_{33}\} + 2\partial_3\{C_{55}\epsilon_{23}\} = 0, \tag{19}$$

$$2\partial_1\{C_{55}\epsilon_{33}\} + 2\partial_2\{C_{55}\epsilon_{23}\} + \partial_3\{C_{13}\epsilon_{11} + C_{13}\epsilon_{22} + C_{11}\epsilon_{33}\} = 0, \tag{20}$$

where the symbols ∂_1, ∂_2, ∂_3 represent the differential operators in the x, y, and z direction, respectively, and where the ϵ_{ij} represent the strains.

Alternatively, for layer 2 we have a similar set of equations but with different coefficients. One may think, therefore, of the governing equations as a system of three, coupled, partial differential equations with sectionally continuous, but constant, coefficients. More specifically, the 3D governing equations become

$$\begin{aligned}\{c_1 + d_1 p(ay)\}\partial_1^2 u + C_{55}\partial_3^2 u + \{c_2 + d_2 p(ay)\}\partial_1\partial_2 v + (C_{13} + C_{55})\partial_1\partial_3 w + \\ + \partial_2\{[c_3 + d_3 p(ay)](\partial_2 u + \partial_1 v)\} = 0,\end{aligned} \tag{21}$$

$$\begin{aligned}[c_3 + d_3 p(ay)]\partial_1\partial_2 u + \partial_2\{[c_2 + d_2 p(ay)]\partial_1 u + [c_4 + d_4 p(ay)]\partial_3 w + C_{22}\partial_2 v\} + \\ + [c_3 + d_3 p(ay)]\partial_1^2 v + [c_5 + d_5 p(ay)](\partial_3^2 v + \partial_2\partial_3 w) = 0,\end{aligned} \tag{22}$$

$$\begin{aligned}(C_{13} + C_{55})\partial_1\partial_3 u + C_{55}\partial_1^2 w + [c_6 + d_6 p(ay)]\partial_3^2 w + \partial_2\{[c_5 + d_5 p(ay)](\partial_2 w + \partial_3 v)\} \\ + [c_4 + d_4 p(ay)]\partial_2\partial_3 v = 0,\end{aligned} \tag{23}$$

where, for the Hercules material system AS4/3501-6, the constants c_i and d_i have been computed as

$$\begin{aligned} c_1 &= 11.241, & d_1 &= -19.179, \\ c_2 &= 0.635, & d_2 &= 0.024, \\ c_3 &= 0.606, & d_3 &= -0.208, \\ c_4 &= 0.635, & d_4 &= -0.024, \\ c_5 &= 0.606, & d_5 &= -0.208, \\ c_6 &= 11.241, & d_6 &= -19.179, \end{aligned} \tag{24}$$

in million pounds (force) per square inch, and where

$$p(ay) = \sum_{n=1}^{\infty} p_n(a_n)\cos(a_n y) \tag{25}$$

with

$$p_n(a_n) = \sin(a_n h)/(a_n h); \quad a_n = n\pi/(2h). \tag{26}$$

This general approach of using a Fourier series to describe the inhomogeneity of the material makes it possible to model many different material systems. By picking appropriate series, one may describe layers of different thickness, layers with glue between the layers, as well as layers of completely different material.

5. Solution

The 2D solution of a single orthotropic layer containing a through the thickness crack was studied analytically first by Ang and Williams (1961) and later by Wu (1968). Subsequently, the 3D case of an isotropic, cracked, plate has been studied, analytically, by Folias (1975). Folias has shown that, throughout the interior portion of the plate, the stress field is proportional to $r^{-0.5}$, and that as one approaches the free surface of the plate, a boundary layer effect is shown to prevail. Furthermore, the thickness of this boundary layer is, in general, less than 5% of the overall plate thickness. Moreover, it was shown that, in this vicinity, all terms, including the R_n terms (where the symbol R_n, stands for higher order terms that do not contribute to the $r^{-0.5}$ stress singular behavior), contribute to the local stress field within this boundary layer. Thus, in such regions, the stress singularity may indeed be different from that which is present in the interior region. In the field of fracture mechanics, the strength of the stress singularity, in such neighborhoods, is still *an open question*. The reader, however, may find in the existing literature some information on the subject (see e.g., Wilcox, 1976; Rosakis et al., 1988; Folias, 1975, 1988b).

Similar trends are also expected to prevail in the present analysis of laminated composite plates. More specifically, in the interior portion of each layer the stress field is expected to be proportional to $r^{-0.5}$, and that as one approaches an interface between two adjacent laminae the stress singularity will change. It may be emphasized, however, that the latter condition is only applicable in a very small spherical region with center at the point where the crack tip intersects the interface (see Figure 3). Its radius r is much less than 5% of the layer thickness. It is now well recognized by the fracture community that the stress singularity in such regions must satisfy the condition of local finite energy, a condition which permits stress fields of the form

$$\sigma \sim p^{-a}; \qquad 0 \leq a < 1.5. \tag{27}$$

Wilcox (1976), in his benchmark paper, proved that if a 3D stress solution satisfies the condition of local finite energy, the solution is unique. In the special case of 2D problems, the condition of local finite energy implies that all displacements will be finite and in fact proportional to $r^{l/2}$. For this limit case, Wilcox's theorem provides the same results predicted by the 2D theorem of Knowles et al. (1973). Alternatively, in the case of 3D problems, the displacements are allowed, at a finite number of points, to be infinite provided that the local strain energy is finite. This is analogous to the 2D fact that stresses are infinite in the immediate vicinity of the crack tip. Physically, a stronger stress singularity suggests that linear

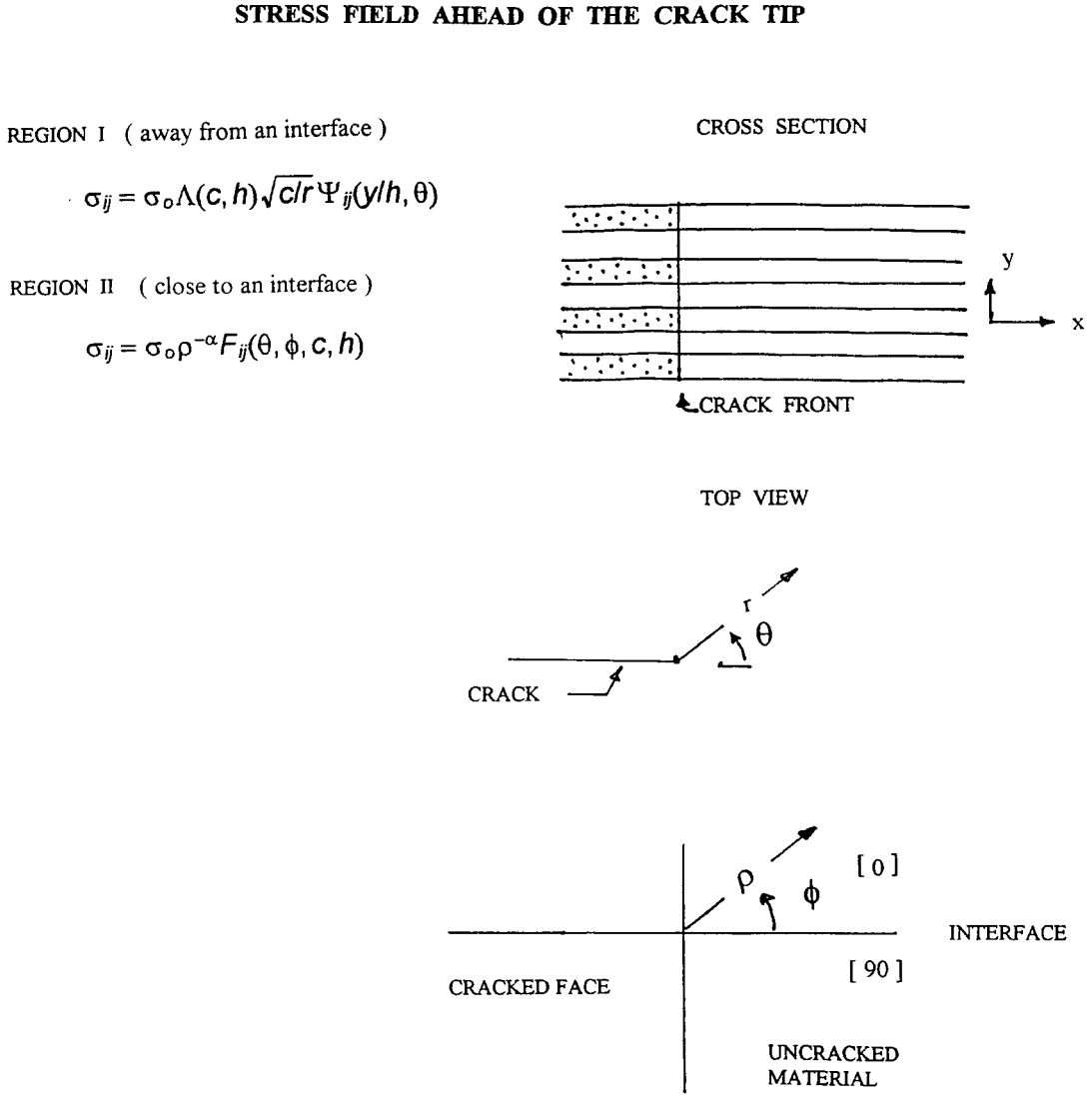

Figure 3. Local coordinates at a ply interface.

elasticity is inadequate in predicting the actual physical behavior of the material per se in such neighborhoods. For example, the solution of a concentrated point load on a half space (Boussineq's problem) gives displacements which are proportional to ρ^{-1} in the neighborhood of the point of application. However, this does not prohibit us from using the solution to extract important physical and practical information, for the simple reason that the neighborhood of its applicability is very small. Moreover, at such interfaces the material has chemically been altered anyway due to the chemical bonds that have taken place. The reader may also note that terms of the form $\sigma \sim \rho^{-a}$ will not. contribute to the total strain energy, as long as a is not equal to -1 or $-1/2$. Thus, for the development of a fracture criterion, we are only interested in the contributions that come primarily from the interior solution. This solution, however, must incorporate the layer thickness correction effect. Moreover, the interior solution in the

neighborhood of the intersection of the crack front and an interface, represents the first and dominant term of the local solution. This is because, as previously noted, other terms such as

$$\sigma \sim r^{(n-0.5)}; \quad n = 0, 1, \ldots , \tag{28}$$

also contribute to the same order of the local stress singularity a. The actual determination of the stress singularity is beyond the scope of this paper and for this reason will he suppressed. However, in view of the work of Folias, (1975), it is expected to be different and most likely higher in its value. This may also be deduced from the implications of the two uniqueness theorems, for 2D (Knowles, 1970) and for 3D (Wilcox, 1976). If the singularity was to be smaller, why is it then that the 3D uniqueness theorem allows higher order stress singularities? After all, 2D elasticity theory is only a special limit of 3D elasticity theory! Additionally, the work of Folias (1992b) perhaps also provides additional support of this conjecture by association. Be that as it may, this subject is beyond the scope of this paper. Numerical methods, such as FE, in general are not valid in such boundary layer regions and usually bypass such difficulties by simply averaging the adjacent points. Moreover, neither can such methods capture the order of the local prevailing stress singularity.

Thus, following the solution of an isotropic layer (Folias, 1975), in conjunction with the work of Walker and Folias (1992), we may now construct Fourier integral representations for the *complimentary* displacement functions u, v, and w which are valid throughout the composite plate (see Appendix). From this general solution we may next construct the following asymptotic expansions, which are valid within the immediate vicinity of the crack tip,

$$u = c\Lambda \sum_{k=0}^{\infty} \int_0^{\infty} \frac{J_{k+1}(sc)}{s^{k+1}} \{A_1^{(k)} \exp(-\beta_1 s|z|) + A_2^{(k)} \exp(-\beta_2 s|z|)\} \sin(sx) \mathrm{d}s + R_n, \tag{29}$$

$$v = c\Lambda \sum_{k=0}^{\infty} \int_0^{\infty} \frac{J_{k+1}(sc)}{s^{k+2}} \{B_1^{(k)} \exp(-\beta_1 s|z|) + B_2^{(k)} \exp(-\beta_2 s|z|)\} \cos(sx) \mathrm{d}s + R_n, \tag{30}$$

$$w = \pm(-c\Lambda) \sum_{k=0}^{\infty} \int_0^{\infty} \frac{J_{k+1}(sc)}{s^{k+1}} \{C_1^{(k)} \exp(-\beta_1 s|z|) + C_2^{(k)} \exp(-\beta_2 s|z|)\} \cos(sx) \mathrm{d}s + R_n, \tag{31}$$

where the symbol R_n stands for higher order terms that do not contribute to the $r^{-0.5}$ stress singular behavior, and where the coefficients $A_1^{(k)}$, $A_2^{(k)}$, $B_1^{(k)}$, $B_2^{(k)}$, $C_1^{(k)}$, $C_2^{(k)}$ are functions of the Fourier integral parameter s and of the geometric coordinate y. For our specific material example, these are given by the relations

$$\beta_1 = 3.3784 - 3.7881 p(ay), \qquad \beta_2 = 0.4317 - 0.4840 p(ay), \tag{32}$$

$$\begin{aligned}
A_1^{(0)} &= -0.2005\sigma_0 - 0.3420\sigma_0 p(ay), \\
A_2^{(0)} &= \quad 0.0463\sigma_0 + 0.0790\sigma_0 p(ay), \\
B_1^{(0)} &= \quad 0.0000\sigma_0 + 0.0000\sigma_0 p(ay), \\
B_2^{(0)} &= \quad 0.0000\sigma_0 + 0.0000\sigma_0 p(ay), \\
C_1^{(0)} &= \quad 0.0104\sigma_0 + 0.0117\sigma_0 p(ay), \\
C_2^{(0)} &= -0.3534\sigma_0 - 0.3962\sigma_0 p(ay).
\end{aligned} \tag{33}$$

(For the sake of convenience in typing the present paper, we have restricted the numerical accuracy of the above relations to four significant figures). Also in writing the asymptotic expansions for the complementary displacements, i.e., Equations(29)–(31) a great deal of knowledge and information has been utilized from past works on the method of solution of singular integral equations as well as on the method of solution of mixed boundary value problems, which Folias has previously developed for the solution of cracked pressurized vessels. Again it should be emphasized that, the asymptotic representations above, are valid only in the vicinity of the crack tip and that when the crack front meets an interface lay-up, there it represents only the first, yet dominant, term of the local solution.

By construction, the above complementary displacement field satisfies the governing equations, the boundary conditions on the faces of the crack by negating their respective contributions from the particular solution, i.e.,

$$\sigma_{zz}^{(p)} = \begin{cases} \sigma_0^{[90]}; & h < y < 2h, \\ \sigma_0^{[0]}; & 0 < y < h, \end{cases} \quad \text{periodic} \tag{34}$$

$$\tau_{xz}^{(p)} = \tau_{yz}^{(p)} = 0; \quad z = 0; \quad |x| < \infty; \quad |y| < \infty \tag{35a,b}$$

where

$$\sigma_0^{[0]} = \frac{1}{2h} \int_{-h}^{h} \sigma_{zz\ \text{particular}}^{[0]}\, \mathrm{d}y \tag{36a}$$

and

$$\sigma_0^{[90]} = \frac{1}{2h} \int_{h}^{3h} \sigma_{zz\ \text{particular}}^{[90]}\, \mathrm{d}y, \tag{36b}$$

as well as the continuity conditions on the plane of the crack and ahead of the crack tip. Moreover, at the ply interfaces, it satisfies the boundary conditions on the normal stress σ_{yy} and the shear stresses τ_{xy}, τ_{yz}. For simplicity in this paper, we have approximated the stress component $\sigma_{zz}^{(p)}$, on the faces of the crack to be sectionally continuous in the y-direction. In general, it will also be a function of x, something that the integral equation handles very nicely with a few additional and simple calculations. Thus, the work may easily be extended to also handle a very *general loading* that an airframe panel may be subjected to. This loading conditions are part of the particular solution and correspond to the case of an uncracked panel. For more information regarding particular solutions and complementary solutions the reader is referred to a book on fracture mechanics.

6. The complementary stress field

From the complementary displacement field, it is an easy matter now to compute the complementary stress field.

6.1. Interior solution

Without going into the mathematical details, it is found that the interior, 3D, stress field is proportional to the usual $1/\sqrt{r}$ singular behavior. A 3D plot of the normalized stress σ_{zz} is given in Figure 4. The reader may notice that in all figures the angle θ is given in radians. As

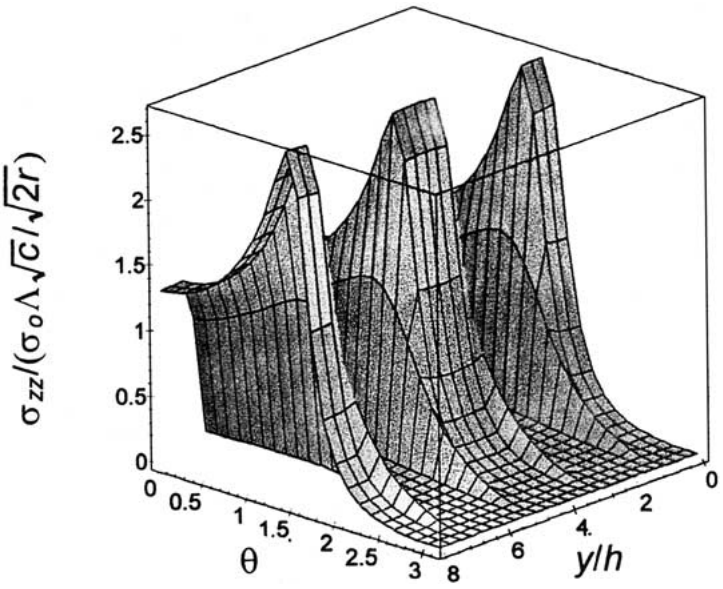

Figure 4. The stress σ_{zz} as a function of (y/h) and θ.

expected, its maximum value occurs in the 0 layer and at a value of $\theta = 83°$, while in the 90 layer its value is relatively low. This suggests, therefore, that fiber breakage is most likely to occur in the 0 layer as a possible mode of local failure. A 3D plot of the normalized stress σ_{yy} is given in Figure 5. Notice that the stress σ_{yy} attains a maximum value at $\theta = 0$ and in the 0 layer. This suggests, therefore, that possible debonding may very well take place in the vicinity of the crack front particularly at the interfaces $y = h, 3h, \ldots$ and on the xz-plane. Debonding, however, may also take place on other planes, e.g., yz-plane. In Figure 6 we plot the stress $\sigma_{\theta\theta}$. Its maximum occurs at $\theta = 0$ and in the interior of the 0 layer, and it vanishes as one reaches the crack face $\theta = \pi$ as it should. In Figure 7 we plot the shear stress $\tau_{r\theta}$, which also vanishes at $\theta = 0$ and at $\theta = \pi$, thus satisfying the boundary conditions, and which attains a maximum at approximately $\theta = 57°$.

Finally, the reader may notice that the stress field changes rather abruptly, in a boundary layer sense, as one approaches the vicinity of the intersection of the crack front and a lay-up interface. This item has been discussed previously and the reader may recall that, in such neighborhoods, the $1/\sqrt{r}$ term represents only the first and dominant term there and that other terms of the form $(r^{(n-1/2)}; n = 0..\infty)$ also contribute to that local stress field. The reader should be cautious in interpreting the previous statement for it does not necessarily imply that the stress singularity there is of the order of $1/\sqrt{r}$. On the contrary, the stress singularity there is expected to be different.

6.2. Exterior solution

Along the crack front and in the vicinity of a lay-up interface, the stress field can be shown to be

$$\sigma_{ij} \sim \rho^{-a} f_{ij}(\theta, \phi, \rho) \tag{37}$$

where ρ, ϕ, θ represent the local spherical coordinates with center the intersection point.

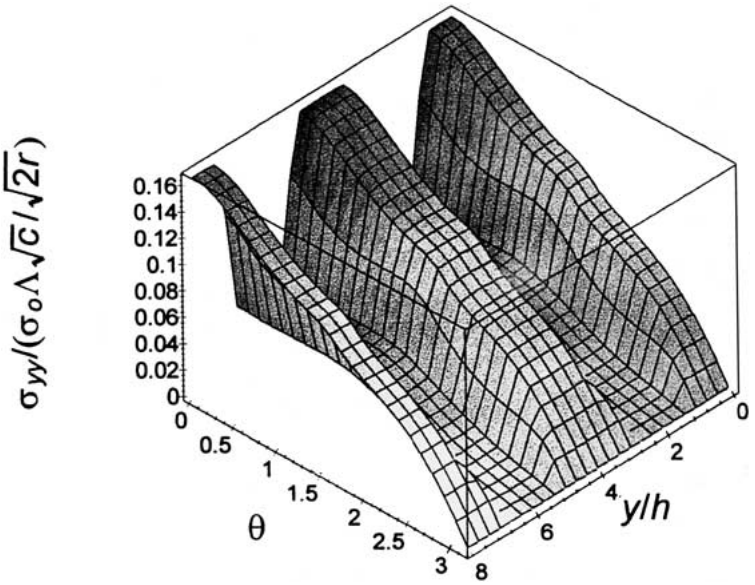

Figure 5. The stress σ_{yy} as a function of (y/h) and θ.

Finally, the function Λ, is determined from the solution of the Cauchy singular integral equation for the stress σ_{zz} over the crack faces. Using the displacement functions given in the Appendix, the stress σ_{zz}, at $z = 0$, may be written after some algebraic manipulations in the form

$$\iint_{\text{crack faces}} \upsilon(\xi, \eta) H(x - \xi, y - \eta)\, \mathrm{d}\xi\, \mathrm{d}\eta = f(x, y), \quad |x| < c, \quad \text{periodic in } y, \tag{38}$$

where the kernel H is a long expression of terms involving modified Bessel K_n functions. The integral equation obtained is similar that of the case of one isotropic layer (Folias, 1980). The details of the method of solution of the above singular integral equation are similar to those developed by Folias for the solution of pressurized vessels containing a line crack (see Folias 1965a,b). Without going into the long and tedious mathematical details, we find

$$\Lambda \approx \left\{1 + 1.55\pi \left(\frac{h_p}{c}\right) - 1.69\pi \left(\frac{h_p}{c}\right)^2 + \cdots\right\}^{O.5}; \quad \left(\frac{h_p}{c}\right) < 0.8, \tag{39}$$

which represents the asymptotic expansion, for very large λ, of

$$\Lambda \approx \left\{1 + 6.90 I_1(\lambda) K_1(\lambda) - 5.28 \left(\frac{1}{\lambda}\right) I_2(\lambda) K_1(\lambda) + \cdots\right\}^{0.5}; \quad \lambda \gg 1 \tag{40}$$

with

$$\lambda = \frac{c}{\sqrt{2}\, h_p}, \tag{41}$$

and where h_p represents the periodic length of the composite material system. The functions I and K represent the modified Bessel functions. It may emphasized that Equation (40) is only valid for very large values of the parameter λ, and that both Equations (39)–(40) are only

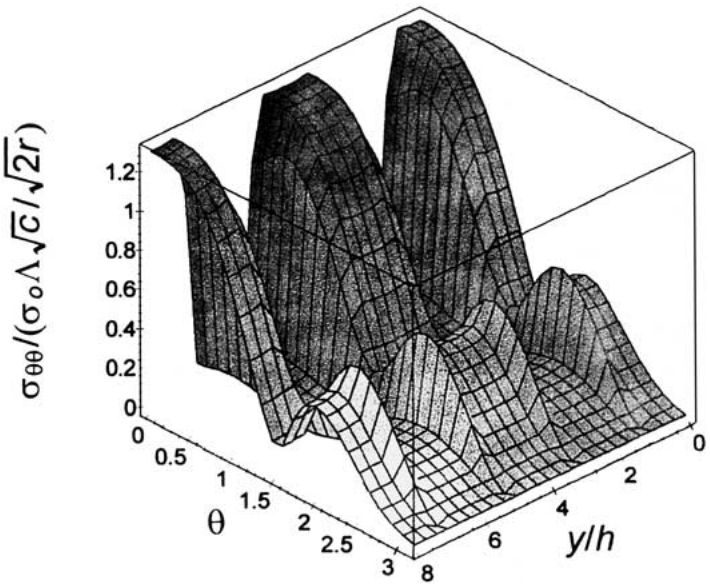

Figure 6. The stress $\sigma_{\theta\theta}$ as a function of (y/h) and θ.

applicable for the material example chosen. Finally, the reader should note that the present analysis assumes that h_p is not equal to zero.

7. Bridging the gap between macro and micro mechanics

As it was noted in the introduction, the damaged zone ahead of the crack tip may be characterized as (i) fiber breakage, (ii) matrix cracking between fibers, (iii) debonding along fiber-matrix interfaces, (iv) matrix cracking parallel to the fibers, (v) delamination along the interface of two adjacent laminae with different fiber orientations, etc. It is now possible to bridge the gap between macro and micro mechanics and thus provide some further insight on the identification of locations where the above possible type of local failures are most likely to occur, why they occur and what their overall effect may be.

For example, by examining the stress σ_{yy} ahead of the crack tip, we notice that the respective locations $y = h, 3h, 5h$ etc., present possible locations where delamination is most likely to take place on the xz-plane. We envision delamination as the debonding of the fiber/matrix interface, followed by cracking of the adjacent matrix, along the last row of fibers as depicted in Figure 11 (Folias, 1991). Thus from Figure 6, and for $\theta = 0$,

$$\sigma_{yy}^{[0]}/\sigma_{yy}^{[90]} = \sigma_{yyply1}/\sigma_{yyply2} = 0.164/0.046 = 3.6,$$

that is a ratio of approximately 4 which suggests that, all things being equal, delamination in layer 1 is most likely to take place than in layer 2.

Finally, both the Tsai–Hill failure criterion as well as the Walker and Thacker (1999) failure criterion will be used in order to predict an overall failure for the composite material system from a global point of view and the two criteria will be compared. It may be noted here that Walker and Thacker have recently shown that the Tsai–Hill failure criterion cannot be used to model anisotropic materials with two strong directions (Yield $= Y$) and one weak direction (Yield $= X$), where $X \leq Y/2$. This is because the geometrical yield surfaces present

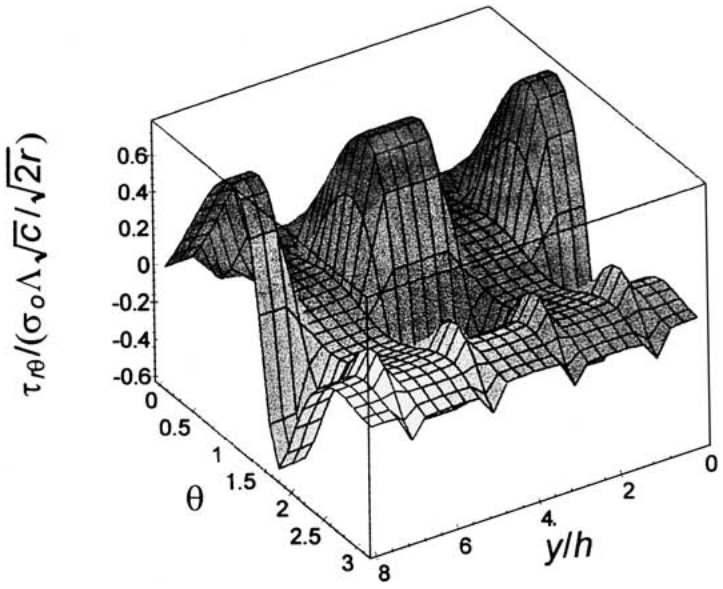

Figure 7. The stress $\tau_{r\theta}$ as a function of (y/h) and θ.

problems. For further discussion on this matter, the reader is referred to the paper by Walker and Thacker (1999). Pending further investigation, the subject matter of bridging the gap between macro and micro mechanics, as well as the two global failure criteria mentioned above, will be the subject of a continuation paper which is to follow.

8. A fracture criterion

It has long been recognized by the fracture community that metal plates, as well as laminated composite plates, which contain, through, flaws or cracks present a reduced resistance to fracture initiation. Consequently, the presence of a flaw or a crack in the plate may severely reduce the strength of the structure and thus cause sudden failures at nominal tensile stresses which may be much lower than the allowable stress. To ensure, therefore, the integrity of the structure, the designer must be cognizant of the relation that exists between fracture load, material properties, flaw shape and size, periodic lay-up orientation, and structural geometry. While the author is very much aware that one fracture criterion may not adequately address the complete failure in a composite material system, it can, however, when integrated with other local criteria provide us with important information that ultimately will help us in better understanding of the phenomenon of damage. Thus, in this section, we will assume that the material fractures in a self-similar manner and will investigate what effect, if any, does the periodic length of the local micro-structure have on the fracturing characteristics of the system. The author strongly believes that the answer to this question is paramount for the complete understanding of failures in composite material systems.

Be that as it may, the principal task of fracture mechanics is precisely the prediction of failure due to the presence of sharp discontinuities. Specifically, the approach is based on a corollary of the first law of thermodynamics which was first applied to the phenomenon of fracture of metals by Griffith (1924). His hypothesis was that *the total energy of a cracked sys-*

tem subjected to an external loading remains constant as the crack advances an infinitesimal distance. That is

$$\frac{\partial U_{\text{system}}}{\partial c} = 0. \tag{42}$$

Thus, following the work of Griffith, we compute the total strain energy of the system, as well as the surface energy. To compute the strain energy, we use the divergence theorem and express the strain energy in terms of the complementary displacement w on the crack faces $z = 0$. Without going into the mathematical details, Griffiths criterion for crack initiation may be approximated by:

$$\sigma_c\sqrt{\pi c}\left\{1 + 1.55\pi\left(\frac{h_p}{c}\right) - 1.68\pi\left(\frac{h_p}{c}\right)^2 + \cdots\right\}^{0.5} \approx K; \quad \text{for} \quad 0 < \left(\frac{h_p}{c}\right) < 0.8, \tag{43}$$

where K stands for the fracture toughness of the composite material system, and $2c$ stands for the size of the crack. Note also that the special case of $h_p = 0$ is meaningless in this analysis. As the ratio of h_p/c increases, more and more terms will be required for a more accurate result. The fracture toughness of the material system is assumed to be a material constant which must be determined by an experiment. A closer examination of Equation (43) suggests the presence of an *effective crack length*, i.e.,

$$\sigma_c\sqrt{\pi c_{\text{effect}}} \approx K, \tag{44}$$

where

$$c_{\text{effect}} = \left\{1 + 1.55\pi\left(\frac{h_p}{c}\right) - 1.68\pi\left(\frac{h_p}{c}\right)^2 + \cdots\right\} c. \tag{45}$$

Thus, the effect of the third dimension, as well as the effect of the local lay-up microstructure along the crack front, increases the actual length of the crack by a factor that is a little larger than c, at least in some region. It is rather instructive to plot the correction factor as a function of the parameter (h_p/c) (see Figure 8). The dotted curve shows the direction which the correction factor appears to go towards as the number of terms increases. Thus, the shape of the curve appears to be, as expected, similar to that of past experimental evidence on cracked aluminum alloy plates (Foreman, 1995), where the fracture toughness now bas been plotted as a function of the ratio (h/c). This suggestion was made by Folias which he based on 3D, linear elastic, fracture considerations and is discussed to some extend in the following reference (Folias et al., 1998).

The above criterion represents a departure from the Mar–Lin theory (Mar, 1977), which is presently used by some to predict failures in laminated composite plates. The Mar–Lin criterion is semi-epmpirical and reads as

$$\sigma_c(\pi c)^m = H_{\text{app}}, \tag{46}$$

where m and H_{app} are two material constants both of which must be determined from experimental observations. Such a criterion, however, suggests that traditional fracture mechanics concepts may not adequately predict failures in laminated composite plates, which may be a little too premature to deduce at the present time. Moreover, different constants m and H_{app} must be determined each time for different material systems

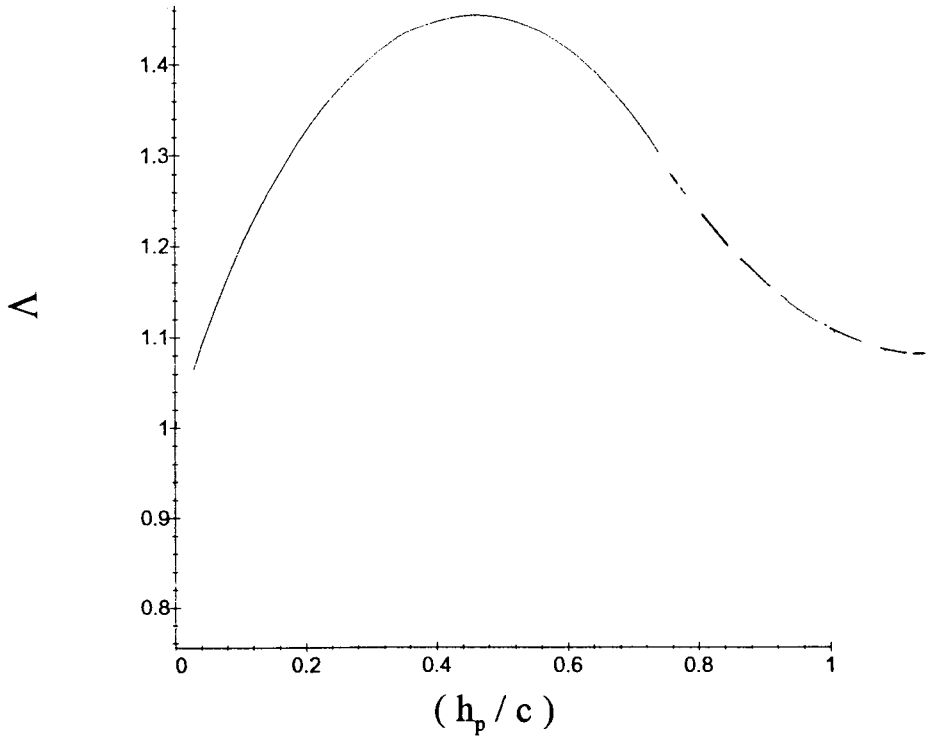

Figure 8. Thickness correction factor for the fracture toughness versus (h_p/c).

9. Comparison between theory and experiments

A theory, in general, is most useful if there exists some experimental evidence to substantiate its validity and its potential use. Thus, in the following, comparisons will be made between some available experimental test data and their theoretically predicted fracture stresses. Although the author has tried very hard to find experimental data for a composite material system with a 0/90 lay-up, he was unable to find any. He was, however, able to find some experimental data of *similar* material systems that will do the job.

Perhaps it may be appropriate here to remind the reader that one of our main goals in this analysis is to establish and substantiate the effect that the periodic length of the local microstructure has on the fracturing characteristics of a composite. While the author well recognizes that, under certain conditions of the material properties, the crack may not advance in a self-similar manner (see Boeing, 2000), however, in order to show the presence of the periodic effect it is best to consider experimental data of a material system that fails in a self-similar manner. Lacking such complete and reliable experimental study, we will use experimental data that are presently available for two slightly different, yet similar, material systems which will do the job. Ultimately, an integrated macro and micro mechanics approach of a composite material system will reveal under what conditions the crack will advance in a self-similar manner or in a manner which presents splitting normal to the crack front. The question of the crack path is not as simple as one may initially think. In general, the author believes the actual path will depend on the material properties, the specific material lay-ups, the different percentages of same lay-ups, the size of the crack, as well as the overall thickness of the composite panel and this is only for mode I loading. Thus, for a failure due to splitting that is

Table 1. Predictions based on Griffith theory Material lay-up: $[45/0/\text{-}45/90]_{2s}$ and $[45/0/\text{-}45/90]_{4s}$

$2c$	h_p	σ_c	exp	K ksi. $\sqrt{\text{in.}}$ no correction	K ksi. $\sqrt{\text{in.}}$ Equation (43)	No. of plies
1 in.	0.044	38.2	ksi.			16
1	0.044	37.8		47.4	55.8	16
1	0.044	42.8				16
1	0.044	40.4				32
1	0.044	39.9				32
1	0.044	38.2				32
2	0.044	32.4				16
2	0.044	29.5				16
2	0.044	34.4				16
2	0.044	28.8				32
2	0.044	29.0				32
2	0.044	28.7		50.9	55.8	16
4	0.044	26.7				16
4	0.044	22.6				16
4	0.044	22.3				16
4	0.044	20.2				32
4	0.044	23.2				32
4	0.044	21.7		50.6	53.4	32

Remarks: The variation of the fracture toughness with no correction factor is 7%, while with correction factor is 4%.

normal to the crack tip, a different failure criterion will be developed, and will be included in a follow up paper.

Be that as it may, the test data were provided by NASA and were carried out by Boeing-St. Louis, on laminated composite panels characterized as high temperature carbon epoxy material systems with a central crack (Boeing, 2000). The fiber volume fraction was approximately 58%, and the dimensions of the outside panel perimeter, relative to the crack, were sufficiently large so that no edge effects will be present. The panels were subjected to a uniform tensile load and the normal stress at fracture was recorded. Unfortunately, the panels that were tested did not have a $[0 / 90]_{2s}$ lay-up. On the other hand, certain panels did have very similar lay-ups. In as much as they were similar and in as much as they failed in a self-similar manner, we will use our derived fracture criterion, i.e., Equation (43), in conjunction with the proper interpretation of the parameter (h_p/c), to predict the corresponding fracture stress. The results are given in Tables 1 and 2. The reader may also note that other panels that were also tested with different percentage ratios of same lay-ups failed in a manner that was perpendicular to the crack front. These data will be used in the continuation paper with an appropriate fracture criterion.

In determining the periodic length, we proceed as follows. First of all, each ply was of 0.0055 in. thickness. Thus, the thickness of the panel for the first entry in the table was

$$2h_{\text{panel}} = 0.0055(\text{number of plies}) = 0.0055(16) = 0.088\text{in}$$

Table 2. Predictions based on Griffith theory Material lay-up: $[45/0/-45/0/0/90/90/45/-45]_s$ and $[45/0/-45/0/0/90/0/45/0/-45]_{2s}$

$2c$	h_p	σ_c	exp	K ksi. $\sqrt{\text{in.}}$ no correction	K ksi. $\sqrt{\text{in.}}$ Equation (43)	No. of plies
1 in.	0.11	42.5	ksi.			40
1	0.11	41.5		52	70	40
1	0.11	44.9				40
1	0.11	45.5				20
1	0.11	49.6				20
1	0.11	45.2				20
2	0.11	34.8				40
2	0.11	33.6				40
2	0.11	32.7		58	70	40
2	0.11	36.7				20
2	0.11	36.6				20
2	0.11	36.6				20
4	0.11	24.8				40
4	0.11	28.8				40
4	0.11	25.9				40
4	0.11	27.4				20
4	0.11	23.8		60	67	20
4	0.11	26.4				20

Remarks: The variation of the fracture toughness with no correction factor is 14%. As the ratio h_p/c increases, so will the variation up to a certain point.

and the corresponding periodic length is

$$h_p = h_{\text{panel}} = 0.088/2 = 0.044.$$

The reader should recall that one may use Fourier series in two different ways. To represent a function that is periodic from $-\infty < y < \infty$ or alternatively, to represent a function from $-h_{\text{panel}} < y < h_{\text{panel}}$, where outside of that interval we do not care what the series represents.

As one can see from the above, as well as from Figures 9 and 10, the agreement between theory and experiments appears to be fairly good. The reader may also notice that for the first material system the fracture toughness is 55.8 ksi$\sqrt{\text{in}}$, while for the second material system 70 ksi$\sqrt{\text{in}}$. This is not surprising for the structure of the latter material system appears to he inherently stronger.

Perhaps it may be appropriate here to make the following two additional comments. First, we believe that only the lowest fracture stress values are of interest in determining critical instability. The rest of it, is experimental scatter. Second, although there is a difference between the material systems $[\ldots]_{2s}$, $[\ldots]_{4s}$ and the [0/90], we have used the same criterion, i.e. Equation (43). The first two materials, by construction, have the same periodicity and as a result should he examined simultaneously. On the other hand, minor changes were anticipated in the fracture criterion between the first two and the third material systems. Perhaps it may be appropriate here to raise the question, why is it that a fracture criterion, which is based

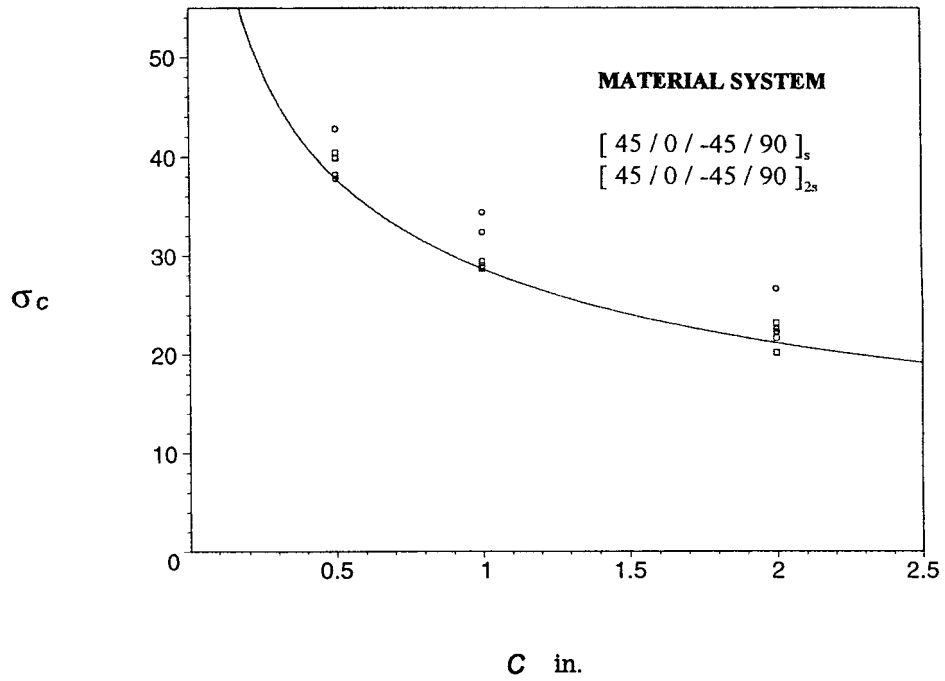

Figure 9. Comparison between theory and experiment of the fracture stress for the material system [45/0/−45/90].

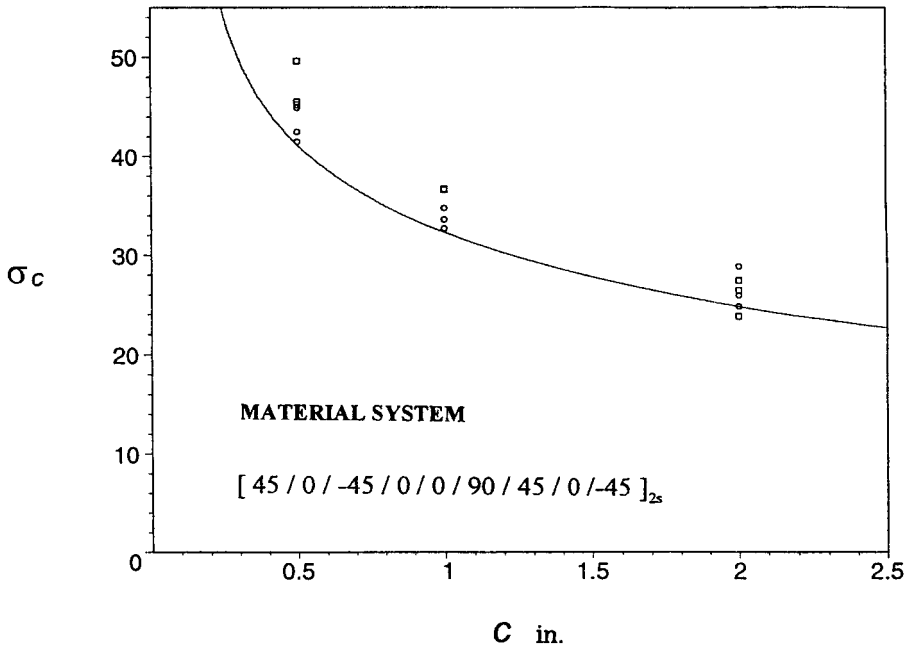

Figure 10. Comparison between theory and experiment of the fracture stress for the material system [45/0/−45/0/0/90/45/0/−45].

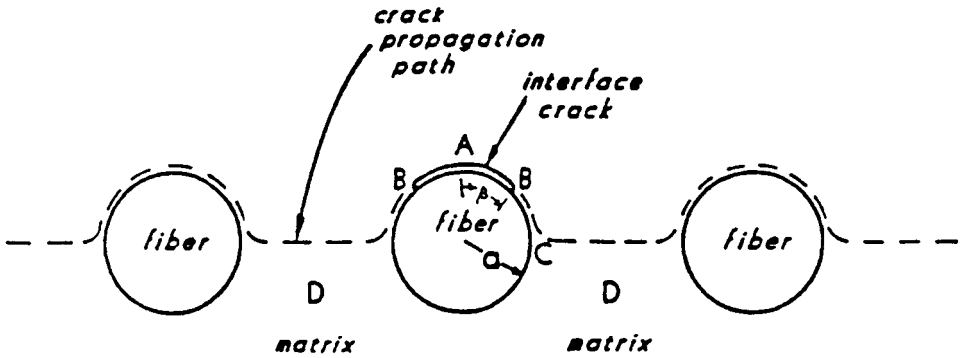

Figure 11. Delamination is modeled as the debonding of the last raw of fibers.

on the derivation of a [0/90] material system, appears to also work for a material system that includes [±45]-layers ? A partial answer to this question is provided on pp. 157–159, of the book by Hellan (1984) and it deals with the effect that the angle of attach between the line of the load and the line of the crack has on the fracture stress. Finally, the reader may also note that in the experimental data there is some experimental scatter of approximately 6% and 8% for Tables 1 and 2, respectively.

10. Conclusions

An asymptotic solution has been constructed in order to determine the effects in the third dimension on the stress field in a laminated composite material system containing a through the thickness, line, crack. The derived stress field, which includes a correction factor that accounts for the effect of thickness, is then used to derive a fracture criterion, similar to that of Griffith, which shows the effect that the periodic length of the local micro-structure has on the fracturing characteristics of the material system. More specifically, the overall effect of the laminate thickness and of the lay-up micro-structure is to increase, in essence, the size of the crack from $2c$ to $2c_{\text{effect}}$. This *effective crack length* is given by Equation (45). Comparison with some available experimental data shows a fairly good agreement and promise.

From this analysis, it is now possible to bridge the gap between *macro* and *micro* mechanics and to provide further insight on the identification of locations where fiber breakage, interface debonding, as well as delaminations are most likely to occur. Pending some further study, this represents the subject of a continuation paper that would follow soon.

Acknowledgment

The work was supported, in part, by NASA, Langley. The author would like to thank Dr. Jim Starnes and Mr. Phil Bogart for this support.

Additionally, the author would like to thank Mr. Phil Bogart, for many valuable suggestions during the write up of the above manuscript, and Col. George Haritos, for many fruitful discussions and for instilling upon the author the importance of the connection between macro and micro mechanics.

Appendix

The complementary displacement functions become

$$u = A_0 + \sum_{n=1}^{\infty} A_n \cos(a_n y),$$

where

$$A_0 = 1/2\{U_0^{[90]} + U_0^{[0]}\} + 1/2 \sum_{v=1}^{\infty} \frac{\sin(\delta_v h)}{(\delta_v h)}\{U_v^{[90]} + U_v^{[0]}[2\cos(\delta_v h) - 1]\}$$

$$\begin{aligned} A_n = & \frac{\sin(a_n h)}{(a_n h)}\{U_0^{[90]} + U_0^{[0]}[2\cos(a_n h) - 1]\} \\ & + 1/h \sum_{v=1}^{\infty} \left\{ \frac{1}{(\delta_v^2 - a_n^2)}[U_v^{[90]} - U_v^{[0]}][\delta_v \sin(\delta_v h)\cos(a_n h) - \right. \\ & \left. - a_n \cos(\delta_v h)\sin(a_n h)] \right. \\ & \left. + \frac{1}{(\delta_v - a_n)} U_v^{[0]}[\delta_v \sin(2\delta_v h)\cos(2a_n h) - \right. \\ & \left. - a_n \sin(2a_n h)\cos(2\delta_v h)] \right\}, \end{aligned}$$

where

$$U_0^{[90]} = -\int_0^{\infty} \left\{ s A_0^{[90]} \exp\left(-\frac{s}{\epsilon_1}|z|\right) + s B_0^{[90]} \exp\left(-\frac{s}{\epsilon_2}|z|\right) \right\} \sin(sx)\mathrm{d}s,$$

$$U_0^{[0]} - \int_0^{\infty} \left\{ s m_1 A_0^{[0]} \exp(-s\epsilon_1|z|) + s m_2 B_0^{[0]} \exp(-s\epsilon_2|z|) \right\} \sin(sx)\mathrm{d}s,$$

and

$$\begin{aligned} U_v^{[90]} = & -\sum_{v=1}^{\infty} \int_0^{\infty} \left\{ s A_v^{[90]} \exp\left(-\sqrt{s^2 + \delta_v^2}\frac{|z|}{\epsilon_1}\right) + s B_v^{[90]} \exp\left(-\sqrt{s^2 + \delta_v^2}\frac{|z|}{\epsilon_2}\right) \right. \\ & \left. + \delta_v C_v^{[90]} \exp\left(-\sqrt{s^2 + \delta_v^2}\frac{|z|}{\epsilon_3}\right) \right\} \sin(sx)\mathrm{d}s, \\ U_v^{[0]} = & -\sum_{v=1}^{\infty} \int_0^{\infty} \left\{ s m_1 A_v^{[0]} \exp\left(-\sqrt{s^2\epsilon_1^2 + \delta_v^2}|z|\right) + s m_2 B_v^{[0]} \exp\left(-\sqrt{s^2\epsilon_2^2 + \delta_v^2}|z|\right) \right\} \\ & \times \sin(sx)\mathrm{d}s. \end{aligned}$$

The remaining complimentary displacements v and w have a similar form. From the above, one may now construct an asymptotic behavior of the displacement field having the proper behavior at the vicinity of the crack. This is given in Equations (29)-(31).

References

Ang, D.D. and Williams, M.L. (1961). Combined stresses in an orthotropic plate having a finite crack. *ARL* **22**, 0–25.

Bakis, C.E. and Stinchcomb, W.W. (1986). Response of thick, notched laminates subjected to tension-compression cyclic loads. *ASTM STP* **907**, 314–334.

Boeing-St. Louis (2000). Tests on laminated composite panels characterized as high temperature carbon epoxy material systems with a central crack. Private communication.

Daniel, I.M., Rowlands, R.E. and Whiteside, J.B. (1974). Effects of material and stacking sequence on behavior of composite plates with holes. *Exp. Mech.* **14**, 1–9.

Ericson, K., Persson, M., Carlsson, L. and Gustavson, A. (1984). On the prediction of the initiation of delamination in a [0/90]s laminate with a circular hole. *J. Compos. Mater* **18**, 495–506.

Folias, E.S. (1965a). The stresses in a cracked spherical shell. *J. Math. Phys.* **5**, 327–346.

Folias, E.S. (1965b). An axial crack in a pressurized cylindrical shell. *I JF* **1**, 104–113.

Folias, E.S. (1975). On the three-dimensional theory of cracked plates. *JAM* **42**, 663–674.

Folias, E.S. (1980), Method of solution of a class of three-dimensional elastostatic problems under mode I loading. *IJF* **16**, 335–347.

Folias, E.S. (1988a). On the interlaminar stresses of a composite plate around the neighborhood of a hole. *I J Solids Structures* **25**, 1193–1200.

Folias, E.S. (1988b). Recent advances on 3D elasticity problems related to fracture. *ASME AMD* **91**, 267–277.

Folias, E.S. (1991). On the prediction of failure at a fiber / matrix interface in a composite subjected to a transverse tensile load. *J. Compos. Mater.* **25**, 869–886.

Folias, E.S. (1992). Boundary layer effects of interlaminar stresses adjacent to a hole in a laminated composite plate. *I J Solids Structures* **29**, 171–186.

Folias, E.S. and Wang, J.J. (1990). On the three-dimensional stress field around a circular hole in a plate of arbitrary thickness. *I J Comput. Mech.* **6**, 379–391.

Folias, E.S. and Bogert, P. (1998). Static Failure in Al 2219-T87 Pressurized Vessels, ASME PVP-Vol. 163, 287–249.

Foreman, R. (1995). Johnson Space Station, private communication.

Griffith, A.A. (1924). The theory of rupture. *Proc. 1st Int. Congr. on Appl. Mech.*, Delft, 55–63.

Hellan, Kare (1984). *Introduction to Fracture Mechanics*. Mc. Graw Hill, New York.

Knowles, J.K. and Wang, N.M. (1960). On the bending of an elastic plate containing a crack. *J. Math. and Phys.* **39**, 223–236.

Knowles, J.K. and Pucik, T.A. (1973). Uniqueness for plane crack problems in linear elastostatics. *J. Elasticity* **3**.

Lekhnitskii, S/G/ (1963). *Theory of Elasticity of an Anisotropic Elastic Body*. Holden-Day, Inc., New York.

Mar, J. (1977). Fracture of boron/aluminoum composite with discontinuities. *J. Compos. Mater.* **11**, 405–.

Pagano, N.J. (1974). On the calculation of interlaminar normal stress in composite laminates. *J. Compos. Mater.* **8**, 89–95.

Penado, F. and Folias, E.S. (1989). The three dimensional stress field around a cylindrical inclusion in a plate of arbitrary thickness. *I. J. Fract.* **39**, 129–145.

Pipes, R.B., Kaminski, B.E. and Pagano, N.T. (1973). Influence of the free edge upon the strength of angle-ply laminates. *ASTM STP* **521**, 218–225.

Raju, I.S. and Crews, J.H. (1982). Three-dimensional analysis of [0/90]s and [90/0]s laminates with a central circular hole. *Compos. Technol. Rev.* **4**, 116–127.

Rosakis, A.J., Ravi-Chandar, K. and Rajapakse, Y. (1988). Analytical, Numerical, and experimental aspects of three dimensional processes. *ASME AMD* **91**.

Rybicki, E.F. and Schmueser, D.W. (1978). Effect of stacking sequence and lay-up angle on free edge stresses around a hole in a laminated plate under tension. *J. Compos. Mater.* **12**, 300–313.

Wang, S.S. and Choi, I. (1982). Boundary-layer effects in composite laminates: Part I. Free-edge stress singularities. *JAM* **49**, 541–560.

Walker, J.D. and Folias, E.S. (1992). Effect of stress waves on laminated composite plates, *I.J.Solids Sructures* **29**, 145–170.

Walker, J.D. and Thacker, B.H. (1999). Yield surfaces for anisotropic plates. In: *Shock Compression of Condensed Matter* (Edited by Furnisch, M.D. et al.) American Institute of Physics, New York, 567–570.

Wilcox, C.H. (1976). Uniqueness theorems for displacement fields with locally finite energy in linear elastostatics. *J. Elasticity* **9**, 221–243.

Wu, E. (1968). *Fracture Mechanics of Anisotropic Plates, Composite Materials Workshop* (edited by Tsai, et al.) a TECHNOMIC publication TECHNOMIC Publishing Co., Inc. 750 Summer St., Stamford, Conn. 06902, 20–43.

Zwiers, R.I., Ting, T.C.T., Spilker, R.L., 1982, On the Logarithmic Singularity of Free-edge Stress in Laminated Composites Under Uniform Extension, *J. Appl. Mech.*, Vol. 49, pp. 561.